Vol. 44(1):39–59
http://dx.doi.org/10.4217/OPR.2022003

Ocean and Polar Research

March 2022

Article

Otolith Microstructural Organization in the South Georgia Icefish *Pseudochaenichthys georgianus* (Channichthyidae) and Cautious Considerations on How Otoliths Can Provide Clues on a Species' Distribution and Migration in Antarctic Waters

Ryszard Traczyk[1] and Victor Benno Meyer-Rochow[2,3]*

[1]Department of Oceanography and Geography, University of Gdańsk, Gdańsk 80-309, Poland
[2]Department of Ecology and Genetics, Oulu University, Oulu SF-90140, Finland
[3]Agricultural Science and Technology Research Institute, Andong National University, Andong 36729, Korea

Abstract : How in the Antarctic icefish, generally, and *Pseudochaenichthys georgianus*, in particular, otoliths increase in size and build new material as the fish ages and passes through different life phases is largely unexplored. Morphometric details of 3418 otoliths of *Ps. georgianus* from S. Georgia and 318 from S. Shetland, were processed and proportions of the amounts of collagen and aragonite removed by EDTA were determined for different age groups. Microstructural investigations showed that characteristics of the 3-dimensinal collagen net are the reason for the radial direction and orientation of the aragonite needles of approximately 1.0 μm in length in larval and 2.3 μm in length in adult specimens. Earlier generated increment layers from the primordial centre (PC) in the dorsal direction restrict those of the secondary centre (SC), causing new growth layer accretion in different directions. In the otoliths of larval *Ps. georgianus*, aragonite layers are 0.89 μm wide while in juveniles and adults they measure 1.45–2.86 μm. Otoliths change from a sphere shape in the larvae to a longish object of irregular outline in the older stages. It is tentaively suggested that the observed otolith shape differences at distinct growth stages are due to physical effects related to swimming speeds at particular water depths and locations. To confirm that otoliths, apart from being useful for age analyses, could also serve to establish correlations between developmental stage and the oceanic environment the fish spend time in, further analyses using additional species and state-of-the-art methods like μCT imaging to evaluate otolith volumes and shapes are required.

Key words : antarctica, ear stones, ageing analyses, aragonite, life stages, vaterite, morpho-functionality

1. Introduction

All teleost fishes possess three otolith end organs, namely the saccule, utricle, and the lagena. Located just below the brain bathed in endolymphatic fluid, of the fishes' otoliths (also known as ear stones) the most easily accessible are the relatively large sagittae of the saccule and the somewhat smaller lapilli of the utricle. The saccule is almost fully encapsulatd by bone in otophysans, whereas it is only ventrally enclosed by bone in most other teleosts. Sacculus and utriculus are involved in head tilts, gravity, linear and to some extent also angular acceleration. The sacculus in particular not only also serves as an organ of hearing in fish, but has retained its ancestral acoustic sensitivity to low frequencies even in mammals (Jones et al. 2010). Otolith applications in fisheries science have been reviewed in detail by Mendoza (2006).

According to Hecht (1987), owing to their species-specific differences in shape, weight and size otoliths are key elements for the identifcation of Antarctic fishes, but they can

*Corresponding author. E-mail: meyrow@gmail.com

also provide approximations of an individual fish's age by relating body length or weight to increases in otolith size. The bones of icefish are largely replaced by cartilage and ice fish skeletons are known to undergo constant metamorphoses (Żabrowski 2000), making otoliths the structures of choice for aging these fishes (Kock 1989; Florin et al. 2018). Sagittae generally show the greatest increase in size as a fish grows and they are therefore the preferred otoliths for aging analyses (Kock 1989; Kellermann et al. 2002). They have helped to identify different life stages and migratory phases in the icefish *Pseudochaenichthys georgianus* (henceforth abbreviated *Ps. georgianus* to distinguish it from the the Antarctic dragonfishes of the genus *Parachaenichthys*) as early as 1980 (Mucha 1980), updated as of late by Kellermann et al. (2002) and Traczyk et al. (2021). Otoliths may be interpreted whole or, more commonly, sectioned into slices aimed to go through their core. The slices are then examined under a light or scanning electron microscope as reported in two recent publications (Traczyk and Meyer-Rochow 2019; Traczyk et al. 2021) that dealt with predictions of *Ps. georgianus'* biomass response to climate change and the species' age structure in different localities.

To interprete or "read" the otolith's annuli from the edge to the core requires a great deal of experience. The fragility of the otoliths, breakages and irregularities in the daily increments along the otolith's growth radius need to be considered and effects of contamination and the replacement of the aragonite by vaterite have to be recognized. Further problems are the frequent lack of knowlege of the amounts and precise nature of the minor components of an otolith's microstructure that could influence the widths of the daily increments. Possible minimum increment widths were first determined by Radtke and Hourigan (1990), based on aragonite crystals. Size, orientation and ability of the otolith's underlying collagen net to stretch, are known to restrict the deposition of aragonite to a suitable percentage with appropriate crystal configuration (Lundberg et al. 2015), thereby determining the shape of the otolith during ontogeny. Size limitations of the daily increments were determined by Traczyk et al. (2020), who confirmed that earlier age estimates of *Ps. georgianus*, based on ototliths, may have had errors owing to the many problems mentioned above associated with interpreting increments in icefish correctly (Mucha 1980). Yet, new problems affecting readings of otoliths have arisen with an increase of contaminants in Antarctic waters and bottom sediments noted since 1999 (Meyer-Rochow 1999; Bargagli et al. 2005; Borghesi et al. 2009; Erren et al. 2013b; Lacerda et al. 2019). High levels of contamination that increase otolth fragility and lead to a reduction in ossification (Żabrowski 2000) and, consequently, holes or perforations in the otoliths (La Mesa et al. 2009; Holcomb et al. 2009), can result in a replacement of aragonite by the less dense vaterite (La Mesa et al. 2009), causing abnormal behavioural patterns in pelagic icefish described as "new behaviours" by Sosiński and Paciorkowski (1993).

Otoliths consist primarily of calcium carbonate ($CaCO_3$) in the form of aragonite in the sagittae and lapilli, but vaterite in the lagenar otoliths (= asterici) (Schulz-Mirbach et al. 2019). A recent study by Justice (2017) has shown that migratory fishes contain higher numbers of individuals that possess otoliths in which aragonite is replaced by up to 50% with vaterite, but that vaterite fish often apparently do not reach their spawning grounds. It has also been shown that sagittae with a higher proportion of vaterite cause hearing impairments in farmed fish (Reimer et al. 2016). Vaterite possesses a hexagonal crystal scaffold, whereas calcite's is trigonal and that of aragonite is orthorhombic. The layers are laid down periodically and leave alternating opaque and translucent bands, whose widths are related to seasonally changing environmental conditions such as ambient temperature, water chemistry and food availablity that a fish encounters during its life (Miller and Hurst 2020). Minor chemical components of the otoliths are elements within the aragonite matrix that reflect to a large extent the chemical composition of the water, but the amounts of trace elements also depend on the fish's diet and water environment. In some cases carbon/oxygen isotope ratios can help identify a species' different juvenile and adult habitats (Meyer-Rochow et al. 1992). Otolith oscillations generate shearing forces that deflect the bundles of the stiff stereocilia of the hair cells of the macula that an otolith is resting on either towards or away from the cell's kinocilium, causing respective depolarization or hyperpolarization responses (Schulz-Mirbach et al. 2019). Responses are sent via the 8th cranial nerve, often referred to as the vestibulocochlear nerve, to distinct regions of the fish brain's medulla where further action may be initiated (Tomchik and Lu 2005).

Because of the importance of otoliths in fish generally (Hawkins and Popper 2018) and *Ps. georgianus* in particular, a detailed analysis of the otolith's microstructure seemed essential to fully understand its role in the different life phases of this, and by extension, other Antarctic species, especially

when we consider the environmental changes that the fish experience when they change from inshore to offshore and then spend a considerable part of their lives on the edge of the continental slope. Towards this end and as a follow-up to our previous publications on icefish otoliths (Traczyk and Meyer-Rochow 2019; Traczyk et al. 2020, 2021), a description of the structural components of *Ps. georgianus*' otoliths, their sizes, shapes and orientations as well as their daily increments seemed desirable and forms the core of this paper.

2. Material and Methods

Collecting field samples

As reported by Traczyk and Meyer-Rochow (2019), specimens of *Ps. georgianus* were collected on several summer cruises to the Antarctic Peninsula and South Georgia between 1976–1991. Collections made at that time by the international science teams of the various research ships involved, met the recommendations later epressed by Reid (2017) and Agnew et al. (2017), officially ratified by CCAMLR (2019). The captured fish were measured and weighed, and their sagittal otoliths were removed and stored under dry conditions. As to the total number of otoliths investigated we can state that 3418 came from specimens of *Ps. georgianus* from South Georgia and 318 (for comparative analyses) from *Ps. georgianus* individuals caught off the South Shetland islands. Body mass and total body lengths were recorded for all individuals of both populations; 1712 otoliths were used in growth pattern analyses and shape changes related to transverse, median, and horizontal planes and 754 for microstructural examinations (e.g. growth stages 0 = 171; I = 64; II = 167; III = 207; lV = 96; V = 43; VI = 6) . A total of 2300 otoliths of *Scomber japonicus* were also available, but they are mentioned in this paper only briefly in the Discussion in connection with otolith fragility and shape relationships.

Given that the analysed material stems from sampling several decades ago and that μCT devices to obtain precise data on the otolith volume were not availabe to scan whole otoliths prior to sectioning or grinding, the formulae available to us to determine volume estimates can, however, be deemed acceptable. Otolith density was calculated from two different measurements, i.e. otolith mass and otolith shape that give a close estimation of otolith volume for near spherical otoliths like those of the larval fish of age group 0. This allowed us to determine a theoretical density value of 0.0029 g · mm^{-3}, which is close to aragonite. By using this larval figure for older fish otolith volumes, we obtain a similar result of high aragonite density. Otolith shape data used in Figs. 3 and 4 of this paper are all based on detailed measurements of circularity, available from Table 3 in Traczyk et al. (2021).

Laboratory Procedures

In the laboratory each sagittal pair of icefish otoliths, coated by a yellowish layer of organic material that does not come off during extraction and cannot be disconnected from the otolith's surface simply with water, was freed from this extraneous material through an immersion in Clorox (5.25% sodium hypochlorite for up to about 1 minute) until exhibiting a white surface to expose the otolith's aragonite body for daily increment readings (Fig. 1a–g). The otoliths were then rinsed in water, dried, and weighed to an accuracy of ± 0.001 mg. Otoliths were chosen as the most suitable structure for age determinations based on the known relationship between otolith and body size. The valuable and reliable method used by Radtke and Hourigan (1990) to study icefish otoliths was used. Their microstructural analysis was based on three principles:

1. To determine the mass of an otolith the latter was weighed and measured and to obtain its volume in the adults an equation based on a regular sphere around the nucleus and with averaged radii (radii in the two directions grow at different speeds leading to an increase in one and a relative decrease in another) was used. Regarding percentages of the main components, the proportions of the amounts of collagen and aragonite removed by EDTA was made use of.
2. To study the degree of the oscillating components of the otolith's daily rings that interact with the frequencies of the vibrational disturbances through inhibiting or facilitating microincrement accretions, maxima and minima of the daily increments were determined on the basis of tropocollagen amount, its space conformation and arrangement of aggregates (Wróblewski at al. 1983).
3. To be able to correlate body and otolith shapes in view of the assumed swimming speeds and resistances encountered as part of a strategy to save energy, otolith planes and orientations in the different age groups were recorded.

Microstructure measurements

All otolith samples were first observed under the light

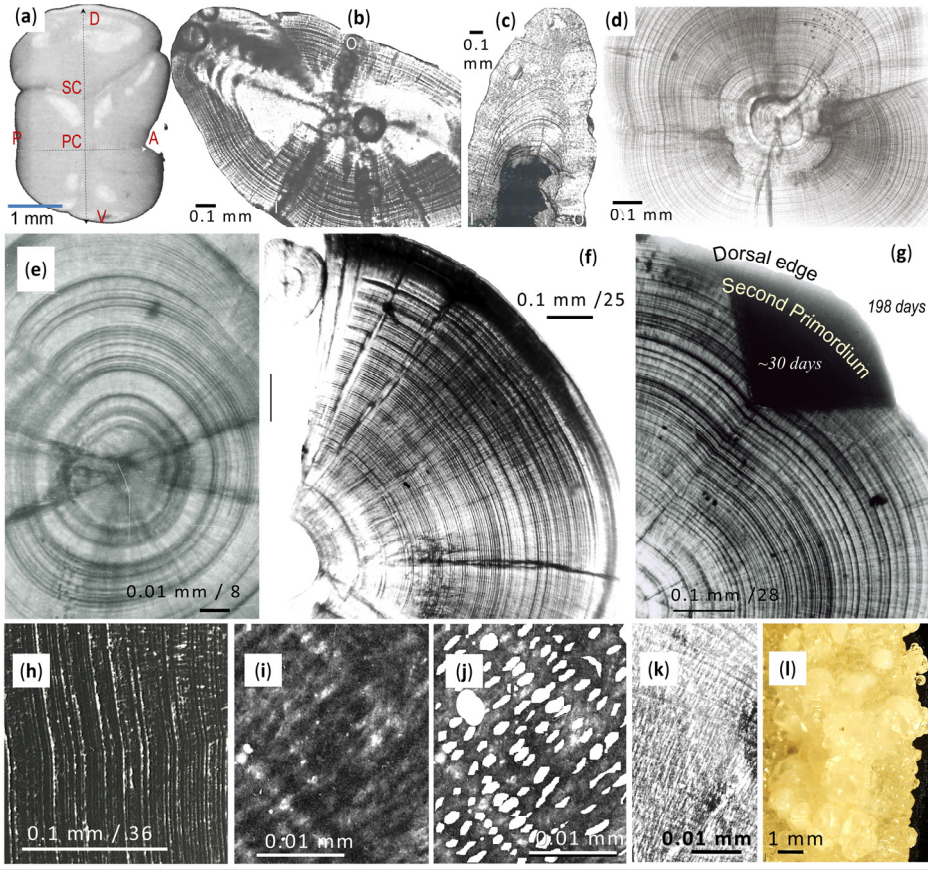

Fig. 1. Morphology and microstructure of the otolith of *Ps. georgianus*. (a) Surface of left otolith with primary centre (PC) indicating where the simultaneous twinning of 4 aragonite crystals commences. Between the PC and the upper (dorsal = D) edge, one more twinning gives rise to a secondary centre (SC). Letters A, P, D, V (i.e. anterior, posterior, dorsal and ventral) refer to the otolith's edges viewed from the inner otolith side. (b) Otolith sectioned along horizontal plane, showing daily increments radiating from twinned PC and becoming increasingly compressed towards the inner (I) and outer (O) sides. (c) Transverse section through the otolith displaying widely spaced daily increments from the SC towards the dorsal edge in contrast to the severely compressed daily increments on the inner and outer sides from the PC. (d) Otolith section along the median plane showing daily increments radiating from the twinned PC. (e) Section along median plane of larval otolith showing that increments radiate from the twinned PC. (f) Otolith section along median plane showing that groups of daily increments can become detached as the otolith increases in size. (g) Otolith section along median plane, showing daily increments at dorsal edge with start of SC with about 30 daily increments from 8 cm TL larvae. (h) Scanning electron micrograph of a transversely cut otolith, showing daily increments but no collagen net. (i, j) Only at higher resolution the pattern of daily increment rings reveals the porous nature of the collagen net, which represents a scaffold-like structure with gaps of about 2.74 µm and collagen net fibres of about 0.8 µm in diameter. (k) Otolith section, revealing an asbestos structure of aragonite crystals linked not only to layers side by side but also radially across daily increments. (l) Otolith surface formed by vaterite crystals that differ from the smooth and streamlined ones formed by aragonite

microscope, cf., Geissinger (1976). The spatial component of the otolith's collagen skeleton was investigated by scanning electron microscopy (Gabriel 1982). Selected larger otoliths were embedded in epoxy resin and sectioned with a low-speed stone saw through the nucleus along frontal and median sagittal plane. Transverse sections of otoliths obtained in this way as well as small but non-sectioned otoliths were mounted in Eukitt (microscopic mounting medium) directly on microscope slides.

Large, sectioned and small non-sectioned otoliths were ground on both sides using carborundum paper (No. 400–800) and polished with a 1 µm diamond compound by hand and a

grinding machine under water to a thickness of 0.1–0.15 mm. Polished sections that went through the nucleus on the median-sagittal (M-S), transverse (T) and horizontal (H) planes were released from Eukitt with chloroform or xylene.

To reveal incremental patterns in the surface relief of the polished sections the latter were etched for 1–8 min with EDTA to remove aragonite and leave protein and then cleaned with water and dried. The etched otolith surfaces were pressed into acetone-soaked acetate sheets that were dried for 30 minutes and removed from the etched surfaces as a finished acetate replica. Etched otolith surfaces (after taking off the acetate replicas) were additionally coated with platinum and palladium to a thickness of 2 nm under vacuum (9.4×10^{-8} Tr) by using an electric arc current at an angle of 45° (Gabriel 1982; Geissinger 1976). The coated sections were then viewed under an SEM (FEI Quanta FEG 250, max resolution of 3 nm) at a variety of magnifications. Most statistical procedures were done usimg STATGRAPHICS version 5.0 (Anonymous 1991) and Excel (Salim and Thekra 2009).

3. Results

Otolith structure and composition

Based on transversely sectioned otoliths, the microstructure of the latter shows that the daily increments represent two unequal layers: narrow and wide radial increments with respective widths of 0.296 μm (±0.0136 μm, SE = 0.078; insensitive to stretching and squeezing) and 2.34 μm (±0.7 μm, SE = 1.6; with a much larger variation due to the effects of stretching and squeezing). The first, i.e. the narrow layer, consists predominantly of collagen fibres that restrict the widths of the second much wider bipartite layer (Fig. 1g, h, i). The second, wider layer is seemingly richer in aragonite crystals that for identification purposes were removed with EDTA (Fig. 1h and i). According to Jolivet et al. (2008), however, EDTA treatment can affect the distribution of EDTA-soluble and insoluble proteins, with the result that one layer contains more aragonite and the other more organic components. Nevertheless, the described procedure does not lead to a detachment of the narrow collagen layers, because they are connected to earlier collagen layers by collagen fibres that cross and link the widely (by aragonite) separated collagen layers (Fig. 1i and j).

The collagen layers and the collagen fibres connecting them with each other represent the 3-dimensional mesh of the collagen scaffold (Fig. 1b, c, d, i, j) that determines the daily aragonite hexahedron crystals' edge length of 2.34 μm (Fig. 1i; Fig. 2a–e). The otolith sections of *Ps. georgianus* show that not only daily increments are present, but that there is also some asbestos material that forms a lattice in amongst the radially polymerizing aragonite (Fig. 1k) and is assumed to be controlled by the 3-dimensional net squeezing adjoining collagen fibres from different daily increments together instead of separating adjacent aragonite layers (Fig. 1c and k).

Additionally, there may be hundreds of unknown proteins in the otolith as shown by Thomas et al. (2019) for the otoliths of the black bream *Acanthopagrus butcheri*. In the latter, the main proteins identified by Thomas et al. (2019) from quantitative proteomic data to be most likely involved in inorganic material secretion were: Na/K-transporting ATPase and V-type proton ATPase, Band-3 anion exchange protein, Na/Ca exchanger 2 and Calmodulin. The two key proteins, enriched in the otolith and assumed to be in control of nucleation, were a phosphorylated putative Stm (starmaker)-homologue as well as a kinase known to be involved in biomineralization, identified as the extracellular serine/threonine protein kinase. Organization, position and gap size of the 3-dimensinal collagen net are the reason for the radial direction and orientation of the aragonite needles of approximately 1.0 μm in length in larval and 2.3 μm in length in adult *Ps. georgianus* (Fig. 1e–j). Respective contributions to the otolith mass of the first (mainly collagen) and the second (mainly aragonite) layer are at least 4.42% (27% of otolith volume) and at most 95.58% (73% of otolith volume) in young and older, 1+ year old icefish (Fig. 1c, i, j).

Instead of further increasing the widths of the daily increments and thereby increasing only the otolith's dorsal radius as the fish ages, radial increments in that dorsal direction begin to accrue twice the hitherto existing dorsal radius as it has two sets of wider increments from the two incremental growth centres, namely those of the more distant, initial primordial centre (PC) and those, generated at the otolith's dorsal edge from the closer new second centre (SC) (Fig. 1a–c). Earlier generated daily increment layers from the PC into the dorsal direction restrict those of the SC and cause the accretion of growth layers in directions other than those only around the PC.

The empirical measurements available on the collagen net's architecture, dimension and organization responsible for the daily growth increments, made modelling of the spatial role of the collagen net not only possible, but a necessity as there is no possibility to observe the growth

processes directly. Based on the arrangement of extracellular tropocollagen of minimally about 0.276 μm side length (Fig. 2a–d), modelling their aggregation in the endolymph gives a measure for the smallest collagen growth unit, i.e., a 3-dimensional rhombohedron with a side length of about 1.3 μm, which is that of a collagen fibre (Fig. 2b and c). Together with the fibres' diameters of about 0.65 μm one arrives at a radial daily increment width of about 2 μm for larvae that are not actively swimming (Fig. 2d left & right). This assessment is based on: a) an aragonite layer restricted by collagen fibres and the resultant rhombohedron side length of 1.3 μm and b) the layer of thick collagen fibres of 0.65 μm in diameter; thus 1.3 + 0.65 = 1.95 (approximately 2 μm).

Otolith differences between not actively and actively swimming develomental stages

Perpendicular to the dorsal radius are two otolith growth radii, one along the transverse plane and a second along the median plane. Most analyses are on the transverse plane as along this plane the growth of the otolith's right inner radius is perpendicular to the vertical axis with the opposite (= left outer radius) giving a value to the otolith's thickness (inner right and outer left sides of the otolith). An otolith's height is therefore given by the dorsal radius plus the ventral radius on the opposite side. Extremely narrow widths of 0.65 μm (Fig. 1c, Fig. 3a and b) can be seen on orthogonal otolith sides.

In the otoliths of larval *Ps. georgianus*, aragonite layers have a thickness of about 0.89 μm, while in juveniles and adults the layers are 1.45 − 2.86 μm wide (Fig. 1b–h). The otolith's shape change (Fig. 1a–f; Fig. 3a and b; Fig. 4a–e) from a relatively large spherical ball in the larvae to a longish object of irregular outline in the older stages could possibly be a response to the increased vertical and horizontal swimming activities and greater speeds of the older age groups. Changes such as these, which affect different species differently, were found to be minor in small pelagic *Champsocephalus gunnari* (which maintain a larval pelagic strategy as adults and consequently retain a more or less spherical otolith), but noticed to gradually get larger in the preferentially bottom-feeding adults of *Chaenocephalus aceratus* (Fig. 4a), and to become even more pronounced in *Ps. georgianus*. In relation to the latter species, we noticed a tendency of the oldest, largest, and mainly female fish to possess otoliths of somewhat rounder more globular shapes than those of the younger adults, possibly as a response to a return to a predominantly horizontal swimming mode during migration and aggregation near the continental slope (Fig. 3c; Fig. 5a and b).

The basic difference between not actively and actively swimming larvae is that the former do not possess stretched or compressed aragonite while actively swimming fish (juvenile/adult) have both stretched and compressed aragonite. The degree of stretching and compressing is highly variable, depending to a large extent on position in the otolith and speed of swimming as shown by the examples shown in the figures. Both juveniles and adults may have stretched and compressed layers, but it is impossible to exactly characterize differences between them, because they were measured only on predominantly transverse sections (horizontal/vertical/transverse section), but not in various different places of the otoliths. In extreme situations stretched layers could become discontinuous on one side of the otolith as in adult *S. japonicus*. Differences in aragonite layers between juvenile and adults need to be examined in more detail in future investigations.

Otolith density and mass in relation to spatial distribution and behaviour

With X-ray diffraction analysis and Raman microspectrometry not available to us but used by Jolivet et al. (2013), we resorted to characterise the constituent crystals of the *Ps. georgianus* otolith as aragonite, calcite or vaterite in the following way. After the removal of the aragonite with EDTA from an icefish's otolith on a stub and cleaning the specimen with water, small invisible amounts of material remained on the wet surface of the stub. However, within a day (when observed by reflected light microscopy or better still under the SEM) this procedure allowed us to identify the crystals. Compared with those of other icefish and in contrast to those of fast swimming fish in which aragonite hairs can lead to narrow and longer otoliths (Fig. 4 a–e), those present in *Ps. georgianus* icefish seemed indicative of slow swimming strategies with extensive vertical migrations (Fig. 3c). Unlike aragonite, calcite would form crystals with flat tops, i.e. transparent crystals called otoconia and vaterite would form transparent otoliths with very bumpy surfaces (Fig. 1l). The large presence of aragonite, equal to 0.002768 g · mm^{-3} (Table 1), rather than that of other calcium carbonate polymorphs like calcite and vaterite confirms the importance of the otolith's density to *Ps. georgianus* for all age groups, i.e., 0, I, II, III, IV, V, VI. A higher amount of aragonite provides otoliths with a greater density, not achievable by the other polymorphs, because of the lower densities of the latter of

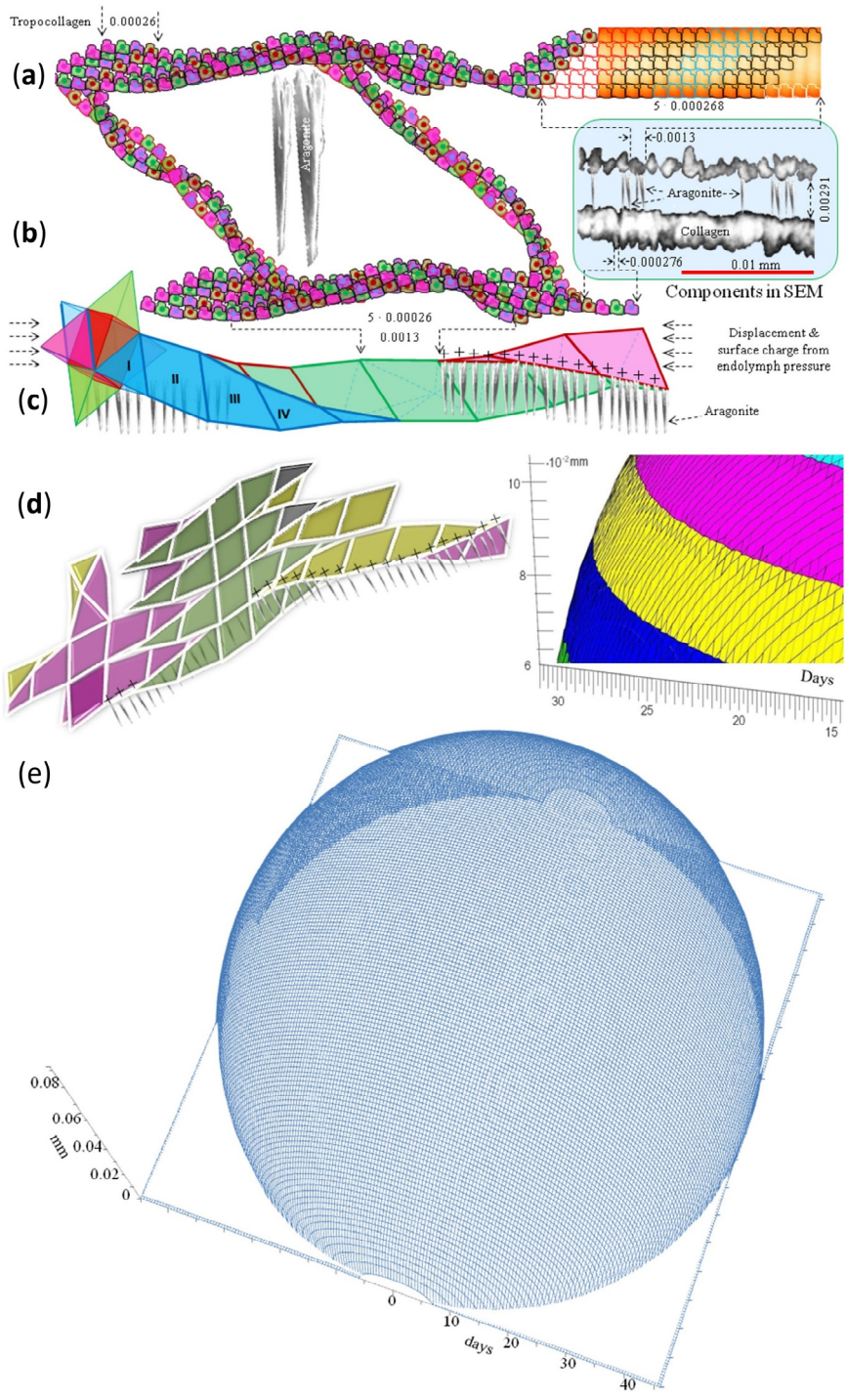

Fig. 2. Semi-schematic depiction of the spatial role of the collagen net with its empirical measurements given in the blue rectangle showing collagen fibres and tropocollagen. (a) Extracellular tropocollagens aggregate into fibres, which, as shown in (b), form rhombus spaces for aragonite deposition. (c) Rhombus-aggregates form rhombohedrons that allow stretching in just any direction and create the rhombohedron space unit of the daily increment. (d) Rhombohedron aggregations forming a new increment layer on the otolith's surface are aided by the power of cohesion. (e) Cohesive forces compel the aggregated tropocollagen net into a sphere under a condition of inactivity (no or little swimming). Theoretically 45 days of increments (representing 0.11 mm and the result of the build-up of 17083 collagen-rhombohedron units around the larval nucleus) of a non-swimming individual produce a pearl-like otolith. The resultant shape is determined by the surface tension under conditions of not actively moving

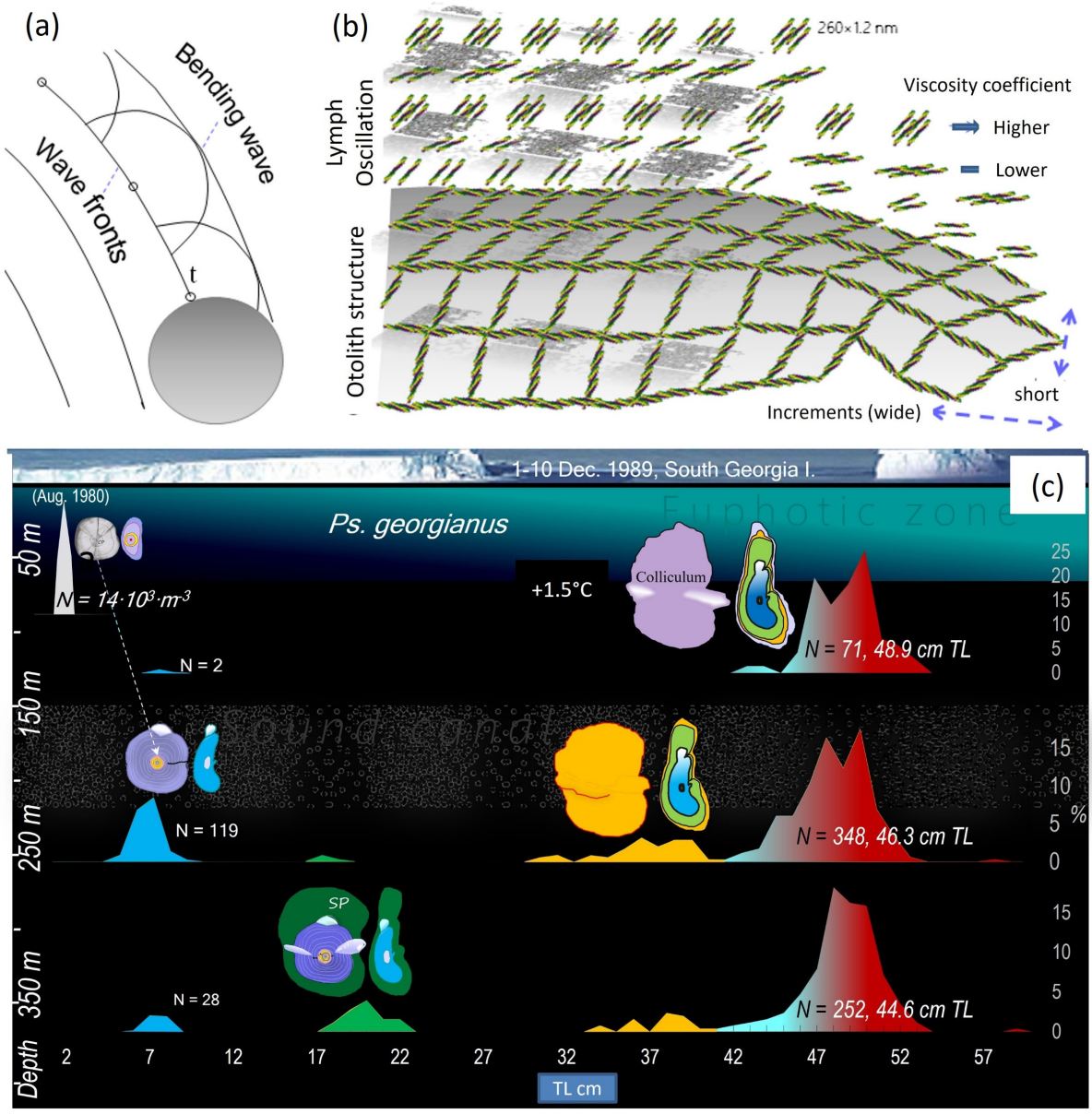

Fig. 3. Accretion of daily layers of rhombohedrons on the otolith's surface and space conformation of aragonite in reference to otolith shapes responding to vertical migrations. (a) Every tropocollagen on the surface of the otolith is subject to vibrations and because of the endolymph's oscillations it can interact with the latter. (b) As the surface increases, tropocollagen layers are forced by Huygens' principle to bend and follow the shape of the earlier surface. During swimming, the formation of a larger otolith surface is governed by the smaller cohesive power and experience of friction that stem from the oscillation of the endolymph. To decrease viscosity, tropocollagens become oriented along the swimming direction with their long axes, thereby leading to an elongation and wider increments of the otolith in the direction of the swimming but narrow increments and shortened otoliths in the perpendicular direction. (c) Early, 5 cm long larvae of August 1980 (upper left) concentrate at depths of about 80 m and have spherical otoliths; 7 cm icefish (middle left), 0 age group larvae migrate to water of about 250 m depth and develop an SC in the otolith; 19 cm young icefish with elongated otoliths occur at the even deeper water of around 350 m (lower left), but 2 year old fish of 33-37 TL return to the shallower depth of around 250 m; larger adults, 45-53 cm (middle and lower right), migrate between 100-500 m. Between latitudes of 50° and 60° (1−10. December 1989, indicated as the location of South Georgia), a vibro-acoustic "channel", affecting otolith growth, is known to exist between the depths of 200 to 400 m. N − number of fish at length class of length frequency. Body length frequencies on the abscissa are indicative of age groups. The left ordinate refers to water depth in m

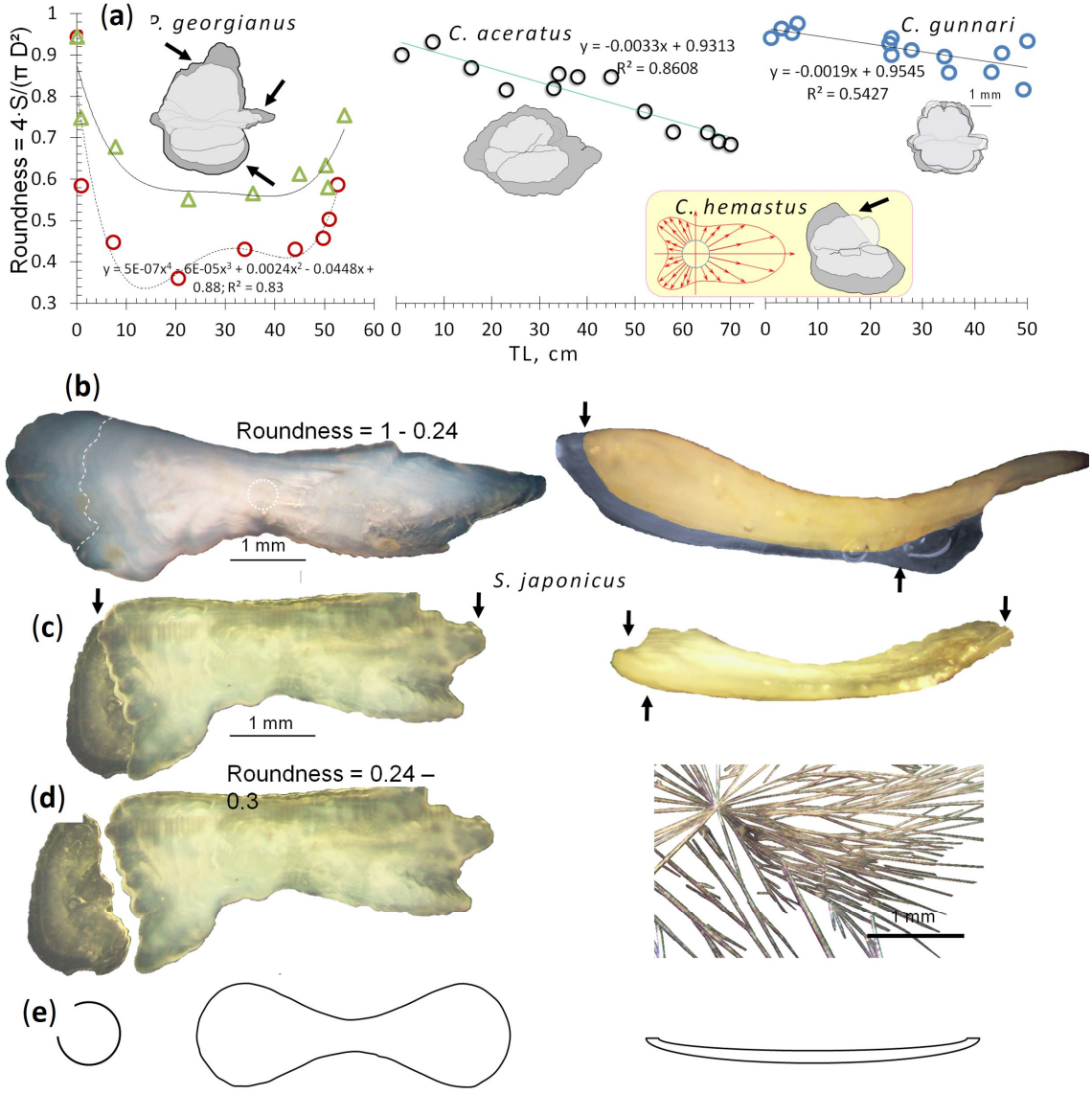

Fig. 4. Comparative changes of otolith shapes during growth from larva to adult in three slowly swimming species of icefish and the fast swimming mackerel *S. japonicus* with noticeable losses of material at the otoliths' edges. (a) Larvae of all species possess otoliths of high sphericity, but in *Ps. georgianus* of 20-30 cm TL otolith sphericity decreases in connection with an increase in vertical migration. Otoliths of larger individuals, however, regain some of their roundness as fish return to inshore larval habitats for spawning. The otoliths' sphericity in *C. aceratus* decreases continually but not to as low as in *Ps. georgianus*, which suggests that adult fish move to the bottom of the sea. In *Ch. gunnari* the otoliths' sphericity decreases very little to only 0.8, which suggests that this species stays in pelagic waters throughout its growth and life. The change of the otolith's shape in *Ps. georgianus* reflects losses of material from the edges indicated by arrows. In the yellow rectangle, arrows indicate axes that determine the contour change of the circle of the liquid crystal substance that slowly moves ahead in one direction and changes the otolith's shape in *C. hamatus* and shows losses off the dorsal edge. (b) In contrast to the otoliths of slow swimming icefish, the otolith shape of fast swimming *S. japonicus* is hugely elongated with its low degree of roundness obtained during development from their originally highly spherical larval otoliths. The dotted line at the posterior edge indicates the otolith's likely fall off region. The otolith of this species on the right shows its very small thickness on the horizontal plane that is further diminished by possible losses on the inner otolith side indicated by arrows. (c) Loss of material from posterior edge, (d) Broken off posterior edge agglutinated to the otolith to maintain some roundness to decrease resistance. On the right, hair-like aragonite from otoliths of *S. japonicus*. (e) Shapes of objects that result in lower resistances to show how otolith shapes can be impacted by swimming speeds

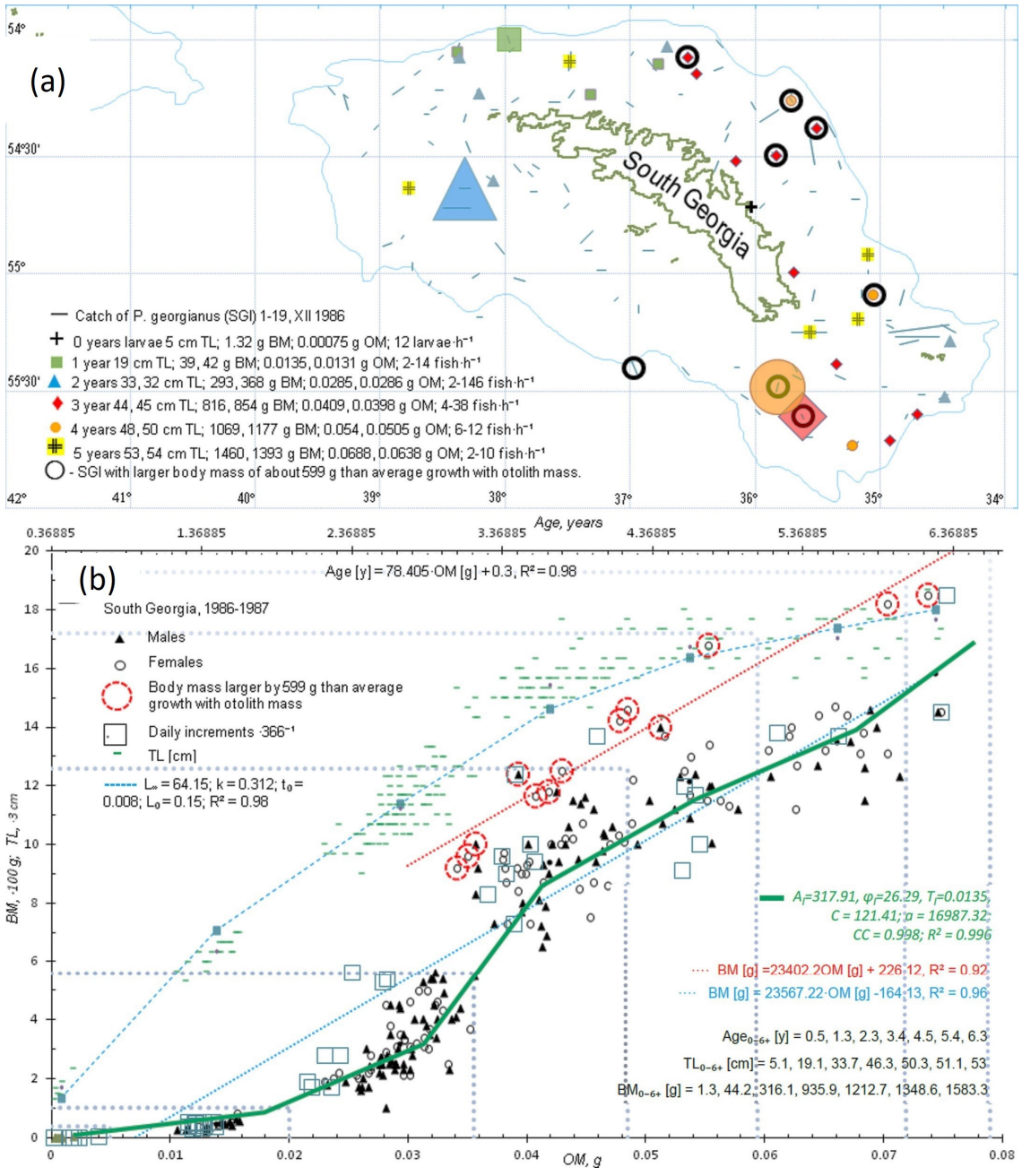

Fig. 5. Horizontal and vertical distribution of development stages (= age groups) of *Ps. georgianus* from larvae to adults. (a) Early larvae, up to 5 cm in length, concentrate inshore near the north-east of South Georgia (Cumberland Bay); young 19 cm icefish concentrate on the western side of South Georgia; 2 year old young, 33 cm long icefish predominate in the south-west of South Georgia, but older adults, 3–6 years old fish with body lengths of 45-53 cm, return for spawning to the north-east of South Georgia. The largest and oldest icefish, mostly females, concentrated near the continental slope in 1986/87. (b) The largest and oldest icefish being mostly females, have a linear and different otolith - body mass relationship (dotted red line and equation on the right) from that of other age groups (dotted blue line and equation on the right). Otolith–body mass relationships explain the periodic equation best that approximates T = 0.0135 g of yearly OM increments. Upper axis is age (years) obtained from otolith mass (bottom axis) by the equation given below. These data, approximated by the Von Bertalanffy relationship (used for all fishery planning), do not in any way show differences between adult icefish with different body and otolith masses occurring near the continental shelf edge.The dotted increasingly larger rectangular regions from the left corner to the right in (b), show age group ranges of body and otolith mass data from the south-west to the north-east region

around 0.00265 g·mm^{-3}. Moreover, together with the much lighter collagen, lighter crystals would reduce the otolith's overall mass and thereby its functionality.

Otolith mass is directly proportional to an icefish's body mass and thereby can be considered body mass driven. The otolith-body mass relationship allows one to distinguish the 5 age groups of *Ps. georgianus* at South Georgia separated by yearly periods of growth between them. Their average lengths at each age group are governed by otolith mass - body mass data. In an average 21 cm TL-fish (= total body length), representative of age group I, we encounter for otolith− body mass values like 0.017−94 g; for 35 cm TL fish (age group II) otolith− body mass values are 0.031−362 g; for 46 cm TL fish (age group III) otolith−body mass values are 0.045−898 g; while respective otolith − body masses for 51 cm TL (age group IV) and 53 cm TL-fish (age group V+) are 0.058−1273 g and 0.068−1579 g (Table 2, Fig. 6a).

Similarly separable age groups, but of lighter mass in the

Table 1. Age classes, fish lengths and body mass, otolith sizes, volume, mass and density of *Ps. georgianus* (SGI) from South Georgia in 1987/88. O. = Otolith, L. collicul = otolith colliculum length (maximum length)

Age Group	Body		Otolith linear dimensions				Otolith cut area		Otolith 3 dim. characteristics			
	Length	Mass	Width	Length	L. collicul	Height	Median	Transv.	Volume	Formula	Mass	Density
Years	cm	g	mm	mm	mm	Mm	mm²	mm²	mm³	mm³	g	g·mm^{-3}
0	7.4	1.01	0.55	1.35	0.66	1.41	1.69	0.99	0.70	$(\frac{1}{3})\pi$ 4R³	0.0020	0.002902
I	20.5	41.1	1.11	2.30	2.09	2.96	5.54	2.34	5.94	2π a·b·c	0.0173	0.002916
II	33.9	348.3	1.48	2.96	3.19	3.82	9.55	4.19	10.98	$(2\frac{2}{3})\pi$ a·b·c	0.0314	0.002984
III	44.1	910.9	1.61	3.48	4.04	4.60	13.44	5.94	16.91	$(2\frac{2}{3})\pi$ a·b·c	0.0444	0.002736
IV	49.7	1242.2	1.87	4.00	4.88	5.25	16.99	8.30	20.56	$(\frac{1}{3})4\pi$ a·b·c	0.0548	0.002668
V	50.9	1380.4	2.13	3.96	5.85	5.78	17.20	10.76	25.55	$(\frac{1}{3})4\pi$ a·b·c	0.0635	0.002484
VI	52.6	1540	2.20	4.22	6.70	5.96	19.35	11.51	29.04	$(\frac{1}{3})4\pi$ a·b·c	0.0780	0.002686

Table 2. Parameters of age groups of *Ps. georgianus* (SGI) from shelf of South Georgia in the summer (XII-II) 1978 with 6 cm long postlarvae recorded

Age group	Otolith mass, g			Body mass, g			Total Length, cm		
	Range	ξ	s	Range	ξ	s	Range	ξ	s
0					4			6	
1	(0.01241-0.02274)	0.01707	0.00228	(65-140)	93.6	16.2	(17-26)	20.9	2.1
2	(0.0269-0.03948)	0.03131	0.00268	(210-605)	362.2	84.2	(30-41)	34.8	2.5
3	(0.04249-0.0472)	0.04476	0.00188	(725-1070)	897.5	121.9	(43-47)	46	1.4
4	(0.04973-0.06598)	0.05757	0.0041	(1000-1620)	1273.3	118.3	(47-53)	50.5	1.2
5+	(0.06517-0.0716)	0.06803	0.00238	(1430-1700)	1578.6	90.1	(50-55)	52.7	1.6

Table 3. Parameters of age groups of *Ps. georgianus* (SGI) from shelves of Palmer Archipelago, South Shetland and South Orkney Islands in the summers of (XII-II) 1978, (XII) 1995[a], and (XII-I) 2006[b]

Age group	Otolith mass, g			Body mass, g			Total Length, cm		
	Range	ξ	s	Range	ξ	s	Range	ξ	s
0							(1-4)[a]	2.3	0.7
1							(15-19)[b]	16.8	0.7
2	(0.02168-0.02766)	0.0245	0.00168	(180-470)	286.3	72.1	(26-39)	31.7	2.8
3	(0.02789-0.03706)	0.03333	0.00191	(520-985)	737.1	90.9	(37-47)	42.4	1.9
4	(0.03485-0.04774)	0.04053	0.00306	(1000-1600)	1255.3	142.3	(39-51)	47.2	2.7
5	(0.04618-0.05377)	0.05102	0.00249	(1470-1790)	1627.9	120	(49-53)	51.3	1.4
6+		0.0619			1750			51	

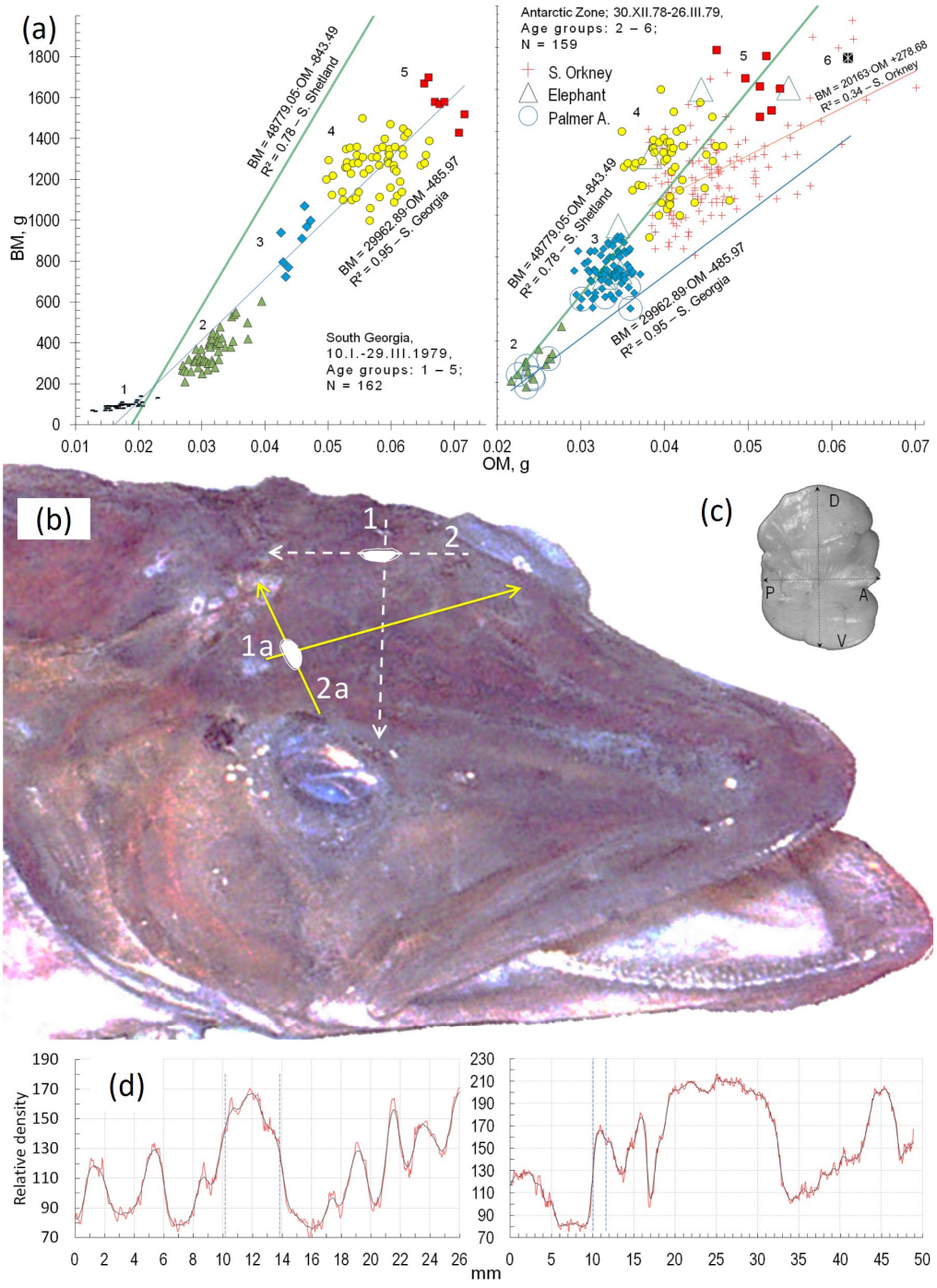

Fig. 6. The otolith functions of maintaining balance and perceiving information on environmental condition lead to two methods to estimate age in icefish (a) Examples of the direct proportional relationship between body (BM) and otolith masses (OM) that define age groups of *Ps. georgianus* in the year 1979 from South Georgia - Subantarctic zone (left) and from the Antarctic zone (right). The different colours indicate different age groups: green triangles = age group 2; blue rhombuses = age group 3; yellow circles= age group 4; red squares = age group 5. (b) Position and ultrasonically identified orientations of *Ps. georgianus*' otoliths in *Ps. georgianus* to obtain the otoliths' lengths (arrows 2 and 2a) and thickness (arrows 1 and 1a) needed for age estimations. (c) Outer side of right otolith. D, V, A, P − dorsal, ventral, anterior and posterior edges of the otolith. (d) Two density profiles of ultrasonically recorded waves that measure maximum otolith length with colliculum (left graph with vertical lines showing anterior and next posterior edge), and otolith thickness (right graph with first vertical line showing outer edge and the next inner edge of the otolith)

Table 4. Parameters of age groups of SGI from shelf of South Georgia in the summer (I) of 1991

Age Group	Otolith mass, g			Body mass, g			Total Length, cm		
	Range	ξ	s	Range	ξ	s	Range	ξ	s
0	(0.00071-0.0037924)	0.00187			4		(6-11)	7.9	
1	(0.009481-0.0227544)	0.01774	0.00228	(65-140)	85	16.2	(15-27)	22.6	2.1
2	(0.0246506-0.0360278)	0.03112	0.00268	(210-605)	362	84.2	(29-40)	35.6	2.5
3	(0.037924-0.0465088)	0.04121	0.00188	(725-1070)	854	121.9	(40-48)	45	1.4
4	(0.047405-0.0587822)	0.05418	0.0041	(1000-1620)	1242	118.3	(47-53)	50.7	1.2
5	(0.0606783-0.0720555)	0.06773	0.00238	(1430-1700)	1344	90.1	(50-53)	50.3	1.6
6	(0.0777441-0.079403)	0.07754			1703		(53-57)	54	

Table 5. Sonic measurements of otoliths, head part dimensions, and body for corresponding age group of *Ps. georgianus*. Otoliths sphericality = 0.7, roundness = 0.5, solidity = 0.95, flatness = 2.4. IW_b − distance between left and right eye (skin width); EyeØ − eye diameter; OM, OH − Otolith Mass and Height; TC Are, TC Pe - Otolith Transverse Cut Area and Perimeter; OL, OT − Otolith Length and Thickness; C Ar, C Pe − Otolith Collagen Area and Perimeter; O_RL − Otolith Rostral Length; SOL, SOT − Sound Otolith Length and Perimeter; Are, Peri − Sound Otolith Area and Perimeter on horizontal plane; CL, CT − Otolith Cyst Length and Thickness; No − Number of sample; TL, SL − Total Length and Standard; BH, BM − Body Heightand Mass; Mat − Maturity Stage; Stom − Stomach content; Spik[n] − Spicules; Vert[n] − Vertebrates; D_1[n], D_2[n] - Rays of first Dorsal Fin and second; $t_1$kv[n] - Rays of Ventral Fin; HL − Length of Head part; IW - distance between left and right eye (bone width)

		Head part			Otolith parameters									Collagen Acoustic				Cyst	
		cm		gram	mm									mm				mm	
	Sex	IW_{bo}	EyeØ	OM	OH	TC Are	TC Pe	OL	OT C	Ar C	Pe	O_RL		S_OL	S_OT	Are	Peri	CL	CT
ξ	♀	4.05	2.924	0.041268	5.10	15.154	16.74												
s		0.17	0.07	0.002539	0.26	1.42	0.774												
ξ	♂	4.14	2.947	0.04351	5.085	15.097	16.58												
s		0.21	0.051	0.003304	0.32	1.489	0.995												
ξ	♀♂	4.09	2.935	0.04236	5.09	15.128	16.67	3.6	1.5	4.9	9.2	4.0		4.93	2.69	10.3	12.8	5.58	3.18
s		0.19	0.062	0.003112	0.28	1.428	0.872	0.1	0.2	0.5	0.4	0.01		0.07	0.09	0.28	0.24	0.01	0.05
Min		3.8	2.8	0.03675	4.41	12.43	14.64												
Max		4.5	3.0	0.04813	5.62	18.49	18.63												

			Body param											Head part		
			cm											cm		
	Sex	No	TL	SL	BH	BM, g	Mat	Stom	Spik[n]	Vert[n]	D_1[n]	D_2[n]	$t_1$kv[n]	HL		IW
X	2	21	46.76	41.86	9.37	1110	3.33	0.67	4.86	53.75	9.24	30.57	22.86	16.48	2.39	4.52
S			2.21	2.24	1.01	190.26	1.32	1.11	0.73	0.44	0.54	0.51	0.36	0.57	0.15	0.21
X	1	19	45.68	41.26	9.27	1097.89	2.21	1.37	4.88	53.42	9.05	30.58	22.68	16.54	2.36	4.56
S			3.42	3.40	0.63	182.96	0.42	1.26	0.60	0.61	0.23	0.69	0.48	0.66	0.17	0.23
X	2,1	40	46.25	41.58	9.32	1104.25	2.8	1	4.87	53.59	9.15	30.58	22.78	16.51	2.37	4.54
S			2.86	2.83	0.84	184.53	1.14	1.22	0.66	0.55	0.43	0.59	0.42	0.60	0.16	0.22
Min			38	33	7.1	780	2	0	3	52	8	29	22	15.3	2.1	4.1
Max			54	49	11.4	1550	5	3	6	54	10	31	23	18.5	2.7	4.9

corresponding age groups (Traczyk et al. 2020, 2021), were identified in *Ps. georgianus* specimens from the Antarctic Peninsula rather than South Georgia with 32 cm TL fish (age group II) and otolith–body masses of 0.0250–286 g; 43 cm TL fish (age group III) and otolith–body masses of 0.033–737 g; 47 cm TL fish (age group IV) and otolith–body masses of 0.041–1255 g; 51 cm TL fish (age group V) with otolith– body masses of 0.051–1628 g; and 51+ cm TL fish (age group VI+) with otolith–body masses of 0.062–1750 g (Table 3, Fig. 6a). Ten to 13 years later the otolith-body mass relationship allows one to distinguish the same 5 age groups of *Ps. georgianus* plus one year younger and one year older groups at South Georgia from 1986 to 1991 as shown, for example, in Fig. 5b and in Table 4.

In this context it is important to mention that average otolith colliculum lengths, O_cL_{III}, were measured for 80 icefish of age group III and determined as 4.04 mm ±0.01, while otolith thickness and head part parameters in the horizontal plane were also recorded (Fig. 5, Table 5). As an otolith's size and shape are species specific, it makes good sense to record body characteristics of a species under investigation in view of future investigations when analysing the changes that the otoliths have undergone during a fish's ageing and location. The respective O_cL_i -values measured by us (with 'i' referring to the age of the group under investigation) for age groups 0, I, II, IV, V, and VI in *Ps. georgianus* were O_cL_0 = 0.66 mm, O_cL_I = 2.09 mm, O_cL_{II} = 3.19 mm, O_cL_{IV} = 4.88 mm, O_cL_V = 5.85 mm, and O_cL_{VI} = 6.7 mm.

4. Discussion

General remarks on underwater acoustics and fish ears

The inner ear of fishes, recently reviewed in detail by Schulz-Mirbach et al. (2019), consists of the three semicicular canals and their ampullae, usually referred to as end organs, which are pouches that contain the otoliths, of which the saccule with its sagitta (the subject of this paper) is the largest. Like the other otoliths, the sagitta is in touch with a sensory pad, known as the macula. The sensory cells of the macula are ciliated and like those of the lateral line organ each possess several stereocilia of different lengths and one kinocilium. The inner ear of fishes can be said to serve several functions: a) to detect angular accelerations that accompany swimming movements and rotations, b) to monitor linear accelerations along rostro-caudal and dorso-ventral axes, c) to determine body position relative to gravity, i.e. to balance the body and d) to register sounds (Popper et al. 2019).

Otoliths in the labyrinth mediate between the acoustic waves of the labyrinth fluid (vibrations of their constituentss) and their receivers - the macula hear hairs. The essence of the otoliths' action is to transfer the energy of the sound waves of the labyrinth's fluid through the structure of the otolith to the next medium of macula composed of sensory hairs leading to an appropriate response. Otoliths, as crystalline bodies of high density and porous structure, absorb, transform and transfer the energy of the sound waves via oscillations in the liquid. The acoustic absorption ability of otoliths depends on their material, porosity, shape and also the geometry of the labyrinth.

To detect local water movements in its near field, a fish has at its disposal also the lateral line system, useful in prey detection under light-deficient environments as, for instance, the deep sea or Antarctic waters in winter and at greater depths. In terms of structural and functional similarities between the lateral line organ, which is well developed in notothenioid fishes, and the stato-acoustic system in fishes, see information provided by Montgomery et al. (1994) and Braun and Sand (2013). As this paper focuses on the otoliths and the latter are ubiquitous and essential structures in fishes generally and icefish in particular, we shall now discuss some aspects of the otoliths' growth mechanics.

Growth of otolith microstructure

In the otolith of *Ps. georgianus* the construction of the radiating scaffold of organic fibres, herewith generally referred to as collagens, is coodinated and alternates with the daily increment pattern of aragonite needles, about 0.00253 mm length, in transverse, median and horizontal planes; thus confirming the earlier observations by Radtke and Hourigan (1990). The daily increments result in accretions of aragonite rings. Their single needles' crystalline nature may have a function to play as a suitable acoustic transducer (Morris and Kittleman 1967; Zhou et al. 2014). The pointed ends of them can be a source of spherical waves (Fig. 3) and possess excellent features for transmissability. The needles' shapes and dimensions would favour the absorption of certain acoustic frequencies (Yang et al. 2020).

The need to remove the organic layer from the otolith's surface with Clorox demonstrates that the new daily increments of the aragonite needles crystalise not directly on the otolith's aragonite surface but in the layer of the organic net covering the otolith's surface. This organic surface cover

contains a meshwork of collagen fibres that are not yet crystalised and represent an aggregated extension of their sub surface net, explaining why cross sections of the otolith's microstructure show that aragonite layers shift in connection with each layer of the collagen fibres in all transverse, median and horizontal planes (Fig. 1). An initial growth of collagenous fibres on the surface of the otolith during the day was reported in the fish *Carapus boraborensis* by Parmentier et al. (2007) and the black bream *Acanthopagrus butcheri* by Thomas et al. (2019). The fibres, 0.15 μm thick, in that species create a net on the otolith's surface, which had pores with side lengths of 2.5 μm, no different from those seen in *Ps. georgianus* (this paper) and thus testifying to the commonalities of otolith growth in fishes generally. Additional support comes from the consecutiveness, i.e. the successsion of collagen layer and aragonite deposition, during the process of aragonization of the otolith's collagenous surface fibre net in *C. boraborensis* (Parmentier et al. 2007), which was also no different from the process in *Ps. georgianus* (this paper).

The precise mechanism of crystal formation and maintenance is not yet fully understood and difficult to research (Lundberg et al. 2015; Schulz-Mirbach et al. 2019). The existence of the radial collagenous scaffold before crystallisation underlines its role first of all in regulating the size and radial direction of the aragonite needles and, secondly, via the elastic fibres of the tropocollagens that make up the network, the control it exerts over the crystallisation process of the aragonite (Sobczak et al. 2003). The arrangement of the tropocollagen net in the endolymph depends largely on vibrations in the environment (Bruus 2012).

Cautious conclusions on the morpho-functinal roles of otoliths

There is indirect evidence that the different otolith morphologies observed in Antarctic fishes are related to the environment (Volpedo et al. 2008) and an earlier rather unsatisfactory attempt to find an explanation was made by Traczyk (2015). The otoliths' shapes have been suggested to possess adaptive physiological features in connection with the fishes' abilities to perceive acoustic stimuli to compensate for the lack of light when at greater depths (Lombarte and Cruz 2007), or a thick layer of ice covers the water's surface or other factors like seasons and a lack of daylight are involved (Volpedo et al. 2008). An elongated laterally compressed otolith shape aligned with the direction of swimming and the inertia of the endolymph, would see to it that endolymph resistance is minimally impacting the otolith (Fig. 3b), favouring pelagic species (Volpedo and Echevarria (2003). However, Lombarte et al. (2010) in an examination of morpho-functional characteristics in Sub-Antarctic and Antarctic nototheniid fishes found that pelagic species had in fact smaller and rounder sagittae than benthic species. These contradictory findings may be the result of different life styles and ontogenies of the species involved. We observed, for example, that age-related otolith shape changes were minor in *Champsocephalus gunnari* (a species that maintained a larval pelagic strategy as adults and therefore retained the small otolith mass and prominent circularity of the larvae), but were more pronouceded in the preferentially bottom-feeding adults of *Chaenocephalus aceratus* (Fig. 4a), and even more noticeable and prominant in *Ps. georgianus.*

Although it is best not to trust theory "until it is confirmed by evidence" (Mac Arthur 1972) or to accept common knowledge until supported by experimental analysis (Erren et al. 2013a), an alternative view has been expressed by Horrobin (1990), who wrote "If a hypothesis which most [scientists or experts] think is probably true does turn out to be true (or rather is not falsified by crucial and valid experimental then little progress has been made. If a hypothesis which most think is improbable turns out to be true then a scientific revolution occurs and progress is dramatic". For Antarctic icefish experimental evidence is hard to come by as icefish are rare and secondly, cannot successfully be kept in aquaria outside the Antarctic. At least for the moment one can only analyse data obtained from specimens of different age groups and locations and draw tentative conclusions based on them. But what is known, is that the sense of vision is better developed in larval and juvenile icefish than in the adults (Miyazaki et al. 2011) and the lateral line organ, too, might be a more suitable sense organ for the larvae to become aware of the approach in the near field of prey and predators alike than olfaction (Montgomery and Macdonald 1987; Montgomery et al. 1988).

Otolith shape change in older icefish and link to geographic distribution: a possible eplanation

As icefish grow and develop a large body size, they sink to sea bottom niches, but every summer migrate again upward into shallower inshore waters for spawning. Icefish do not possess a swimbladder and a decrease in body mass via a large reduction of bone ossification (Żabrowski 2000) is advantageous when the fish ascend from deeper water to the shallower spawning sites. To compesate for the drop in body

mass, females in particular experience less aragonized, lighter otoliths lacking material from dorsal, ventral and colliculum edges. The result is greater otolith fragility in adult *Ps. georgianus* (Mucha 1980) and *Ch. gunnari* (Hecht 1987) (Fig. 4a). Meanwhile owing to the bottom life strategies of *Chaenocephalus aceratus* and *Chionodraco hamatus,* these species exhibit important corrections for the decrease of body mass after spawning, but collicula extending the otolith's margin, as in *Chaenodraco wilsoni* and *Ch. gunnari* (Hecht 1987) are indicative of maintaining a pelagic life.

Ps. georgianus is known to prefer cold water in its wide horizontal geographical and vertical distribution (North 1988; Whitehouse et al. 2008). Its 15–20 mm long larvae found inshore at depths of 0–90 m (North 1990) hatch in the southern winter month of May at South Georgia (Efremenko 1983; Kock and Kellermann 1991). Larvae a few months of age and about 7 cm long and and one year old approximately 21 cm young fish, present mainly in the south west of South Georgia, sink to a depth of 350 m to avoid the warmer summer surface water or predominate in the Antarctic Zone of the colder Palmer Archipelago, where appropriately small-sized food items are abundant and available to them (Traczyk et al. 2020). The formation of an SC that results in a doubling of otolith height (Traczyk et al. 2020) allows icefish a wider range of vertical migrations than if they retained rotund or spherical otoliths at the north east of South Georgia (Fig. 5a) and in the Antarctic Zone at S. Orkney (Fig. 6a). When migrating inshore in April to spawn over the shallow sea bottom to the northeast of South Georgia (Vanella et al. 2005), Kock and Kellermann (1991), Permitin (1973) and Militelli et al. (2015) discovered that the largest adults horizontally migrated to north-eastern offshore regions (Fig. 5a) because of the abunadance of their major krill food, i.e. *Euphausia superba* in that region (Traczyk at al. 2020).

Adult *E. superba* after daily feeding in the warmer surface water descend at night to the colder and darker depths, generating frequencies of 50–200 Hz and 50 $N \cdot m^2$ pressure while they move. *Ps. georgianus*, being largely nocturnal (Jones et al. 2000), feed on krill during the night and using their otoliths should be able to localise the krill as sounds (Sheykholeslami and Kaga 2002; Jones et al. 2010). They may also use their lateral line organ to detect the movements of nearby prey, but there is no evidence that they use olfaction (Montgomery et al. 1988). The largest larval otolith nuclei of all icefish species whose larval otoliths have been examined, are those present in *Ps. georgianus* (as it is this species, whose young hatch earliest in winter and then get transported from icy nearshore to deeper waters). The next smaller otolith nucleus is present in *C. aceratus* whose larvae hatch a little later in early spring, but the smallest nuclei are found in *Ch. gunnari*, a species that hatches in late spring when all the ice has melted and the ice cover has disappeared. In this way the larvae of the three species avoid competition and distribute ecological pressure on different food resources (North and White 1987) and to different regions despite similar depth and sound channel preferences of all icefish species to congregate (Fig. 3c).

The significantly different amounts of otolith masses that permit researchers to distinguish sexes, age classes and ecological groups cannot reliably be assessed with body length data alone. The smaller mass of the otoliths of the largest icefish may have been brought about by absorbed, i.e. eliminated tips along the dorsal and/or collicular edges and losses associated with the establishment of the new SC. As shown in the results of this paper, the biggest individuals of each age group, being mostly female *Ps. georgianus*, exhibited different relationships of body-otolith masses that were based on the lighter otoliths of fish predomonantly from around South Georgia in 1986/87, 1987/88 and 1989/90 (in the earlier years 1977/78 fish were predominantly from only the northeast of South Georgia: Sosiński and Paciorkowski 1993). Similar observations (unpublished) were made on otolith thinning in *C. hemastus* (demonstrable by comparing CCAMLR data of Motta et al. 2009 with the old ones of Hecht 1987) and *Ch. gunnari* (Fig. 4a), the latter in particular a species that leads a pelagic life near the continental slope in which reduced otolith mass and more prominent circularity were characteristic features; features that were shared with *Scomber scombrus japonicus'* highly fragile otoliths (but for the different reason of high speed swimming that provided an even stronger cause of otolith fragility: Fig. 4a). The trend in otolith parameters of the largest adult indivuduals of *Ps. georgianus* to revert to lighter otoliths is likely to be related to the fish's horizontal migration following spawning in shallower water.

5. Conclusions

Microstructural growth patterns of otoliths and the noticeable differences of otoliths at various developmental stages and locations can be regarded (and treated) as independent issues. However, taking into account the structure and

function of otoliths in the lifetime of a fish, the issues are correlated as has been pointed out in the recent holistic approach by Schulz-Mirbach et al. (2019), who showed that developmental and genetic mechanisms, phylogenetic constraints, certain ecological factors and environmentally induced phenotypic plasticity all play some role in how an otolith is built and functions.

By changing the shape of an otolith from a near spherical to a longer shape, resistance decreases can be achieved. However, the shape changes are determined by the underlying microstructure, i.e., the orientation and lengths of the aragonite hairs. For elongations to occur there is thus some "squeezing" of the aragonite hairs into one direction (cf. Fig. 4b–e). These changes affect the microstructure and are predominantly in the transverse and not the median plane (because fish swim in a straight direction and do not move sideways like crabs). The changes depend on swim speed, ambient temperature, depth, water currents, pressure and a species' strategy to obtain food. For example, deep water species like grenadier *Macrourus carinatus* are not fast swimmers, but possess long and flat otoliths because of the high pressure in their environment and a feeding method that does not depend on sudden fast forward bursts.

Changes in otolith shapes are therefore brought about by the otolith's microstructure and that ultimately determines an otolith's functional efficiency (Gauldie 1988). If, for example, vaterite were to dominate an otolith's microstructure, the otolith cannot obtain a suitable shape, because vaterite does not have the orthorhombic shape that aragonite possesses (Zhou et al. 2010). Regular spherical otoliths occur in *Pseudochaenichthys georgianus* prior to hatching from the egg, when swimming speeds are zero. Newly-hatched icefish larvae are swimming at speeds of 0.01 km/h and exhibit otolith changes in the transverse but not the median plane, which results in microstructural squeezing to achieve a reductin in hydrodynamic resistance. In the median plane microstructural changes are absent or minimal as the otoliths do not experience pressures to lessen resistance. One can argue therefore that during ontogeny as the speed of a fish increases from 0 km/h (the situation in the egg) via 0.01km/h (situation in newly hatched larvae) and 0.1 km/h (sitation in inshore larvae) to 0.4 km/h in offshore adults, otoliths adapt (Fig. 7): they change their shapes as a consequence of the microstructural arrangement along the transverse plane from spherical to long and flatter thereby reducing the otolith's resistance in the lymph (cf. Fig. 3b and c).

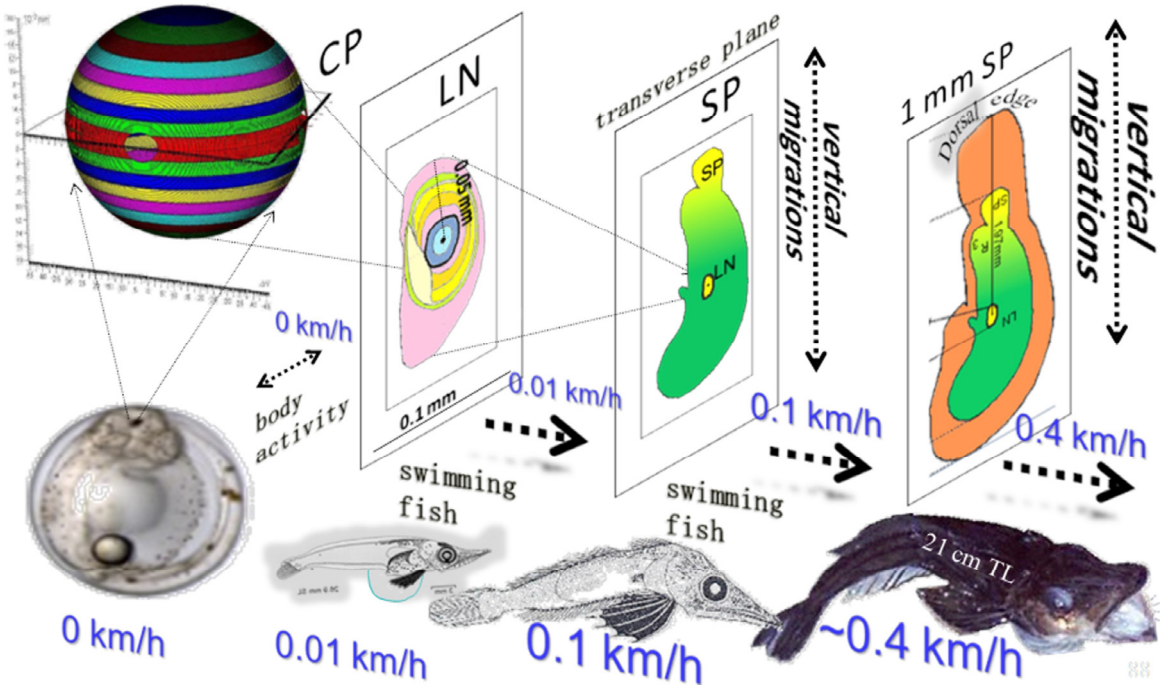

Fig. 7. Growth of a fish and the average swimming speeds that accompany the different developental stages, affect both size as well as shape of the sagittal otolith in *Ps. georgianus*. As swim speeds increase in the larger individuals the otolith changes from a nearly spherical object to a longer and flatter structure. Changes such as these are brought about by the microstructural orientation of the aragonite hair component of the otolith

Since the otolith is the most appropriate structure to estimate an icefish's age from, given the availability of ultrasonic equipment with sufficient resolution, we suggest that it ought to be possible to obtain information not only on an icefish's age but also its developmental stage and oceanic environment without a) having to kill the fish, b) having to extract its otoliths and c) having to consider errors based on lost, detached and separated otolith colliculi or dorsal edge absorptions. Furthermore we could show that to measure otolith length along its horizontal plane for age estimates of adult fish was preferable to taking measurements of an otolith's height as height growth slows down and the otolith's height in the adults eventually completely stops to increase (Traczyk et al. 2021).

Acknowledgments

We thank all those that were involved with the collection of the material, and all who offered help and advice throughout this study. RT in particular further gratefully acknowledges the support received from the Sea Fisheries Institute, Imperial College, University of London, the British Antarctic Survey and the University of Gdańsk. For their hospitality during a brief visit in the Austral summer of the year 2000, VBM-R thanks the staff of Poland's Antarctic Arctowski Base and acknowledges the support received from Professor Chuleui Jung via the Basic Science Research Program of the National Research Foundation of Korea (NRF) funded by the Ministry of Education (NRF-2018R1A6A1A03024862) to complete this study.

References

Agnew DJ, Gutierrez NL, Stern-Pirlot A, Hoggarth DD, (2017) The MSC experience: developing an operational certification standard and a market incentive to improvefishery sustainability. J Mar Sci **71**:216–225

Anonymous (1991) Stratgraphics version 5. Reference manual. STSC, Inc., Rockville, 555 p

Bargagli R, Agnorelli C, Borghini F, Monaci F (2005) Enhanced deposition and bioaccumulation of mercury in Antarctic terrestrial ecosystems facing a coastal polynya. Environ Sci Technol **39**(21):8150–8155. doi:10.1021/es0507315

Borghesi N, Corsolini S, Leonards P, Brandsma S, de BoerJ, Focardi S (2009) Polybrominated diphenyl ether contamination levels in fish from the Antarctic and the Mediterranean Sea. Chemosphere **77**(5):693–698

Braun CB, Sand O (2013) Functional overlap and nonoverlap between lateral line and auditory systems. In: Coombs C, Bleckmann H, Fay RR, Popper AN (eds) The lateral line system. Springer-Verlag, New York, pp 281–312

Bruus H (2012) Acoustofluidics 7: the acoustic radiation force on small particles. Lab Chip **12**:1014–1021

CCAMLR (2019) CCAMLR Statistical Bulletin, Vol 31. Convention on The Conservation of Antarctic MarineLiving Resources. https://www.ccamlr.org/en/document/data/ccamlrstatistical-bulletin-vol-31 Accessed 29 Aug 2020

Efremenko VN (1983) Atlas of fish larvae of the Southern Ocean. Cybium **7**:1–74

Erren T, Koch MS, Meyer-Rochow VB (2013a) Common sense: folk wisdom that ethnobiological and ethnomedical research cannot afford to ignore. J Ethnobiol Ethnomed 2013, **9**:80.

Erren T, Zeusz D, Steffany F, Meyer-Rochow VB (2013b) Oceans of plastics. In: Allodi S, Nazari EM (eds) Exploring themes on aquatic toxicology. Research Signpost Publication, Trivandrum, pp 51–74

Florin AB, Hüssy K, Blass M, Oesterwind D, Puntila R, Ustups D, Albrecht C, Heimbrand Y, Knospina E, Koszarowski K, Odelström A (2018) How old are you - evaluation of age reading methods for the invasive round goby (*Neogobius melanostomus*, Pallas 1814). J Appl Ichthyol **34**:653–658

Gabriel B (1982) Biological scanning electron microscopy. Van Nostrand Reinhold Company, New York, 186 p

Gauldie RW (1988) Function, form and timekeeping properties of fish otoliths. Comp Biochem Phys A **91**(2):395–402

Geissinger HD (1976) Intermicroscopic (LM, SEM, TEM) correlation. In: Hayat MA (ed) Principles and techniques of scanning electron microscopy, Vol 5. Van Nostrand Reinhold, New York, pp 94–121

Hawkins AD, Popper AN (2018) Direcional hering and sound source localization by fishes. J Acoust Soc Am **144**(6):3329–3350. doi:10.1121/1.5082306

Hecht T (1987) A guide to the otoliths of Southern Oceanfishes. South African J Antarctic Res **17**:1–87

Holcomb M, Cohen AL, Gabitov RI, Hutter JL (2009) Compositional and morphological features of aragonite precipitated experimentally from seawater and biogenically by corals. Geochim Cosmochim Ac **73**:4166–4179. doi:10.1016/j.gca.2009.04.015

Horrobin DF (1990) The philosophical basis of peer review and the suppression of innovation. JAMA **263**(10):1438–1441

Jolivet A, Bardeau J-F, Fablet R, Paulet Y-M, de Pontual H (2008) Understanding otolith biomineralization process: new insights into microscale spatial distribution of organic and mineral fractions from Raman microspectrometry. Anal Bioanal Chem **392**(3):551–560

Jolivet A, Fablet R, Bardeau J-F, de Pontual H (2013) Preparation techniques alter the mineral and organic fractions of fish otoliths: insights using Raman micro-spectrometry. Anal Bioanal Chem **405**(14):4787–4798

Jones CD, Kock K-H, Balguerias E (2000) Changes in biomass of eight species of finfish around the South Orkney Islands (subarea 48.2) from three bottom trawl surveys. CCAMLR Sci **7**:53–74

Jones GP, Lukashkina VA, Russell IJ, Lukashkin AN (2010) The Vestibular system mediates sensation of low-frequency sounds in mice. J Assoc Res Oto **11**(4):725–732

Justice J (2017) Converting chemical signatures in vaterite otoliths to aragonite otoliths in steelhead trout: developing a partition coefficient. https://scholarworks.bgsu.edu/honorsprojects/243 Accessed 12 Mar 2018

Kellermann KA, Gauldie RW, Ruzicka JJ (2002) Otolith microincrements in the Antarctic fishes Notothenia coriiceps and Pseudochaenichthys georgianus. Polar Biol **25**:799–807

Kock K-H (1989) Results of the CCAMLR Antarctic fish otoliths/scales/bones exchange system. Commission for the Conservation of Antarctic Marine Living Resource, Hobart, pp 197–226

Kock K-H, Kellermann A (1991) Reproduction in Antarctic notothenioid fish. Antarct Sci **3**:125–150

La Mesa M, De Felice A, Jones CD, Kock KH (2009) Ageand growth of spiny icefish (*Chaenodraco wilsoni* Regan, 1914) off Joinville-D'Urville Islands (AntarcticPeninsula). CCAMLR Sci **16**:115–130

Lacerda ALDF, Rodrigues LDS, van Sebille E, Rodrigues FL, Ribeiro L, Secchi ER, Proietti MC (2019) Plastics in sea surface waters around the Antarctic Peninsula. Sci Rep **9**(1):1–12. doi:10.1038/s41598-019-40311-4

Lombarte A, Cruz A (2007) Otolith size trends in marine fish communities from different depth strata. J Fish Biol **71**(1):53–76

Lombarte A, Palmer M, Matallanas J, Goez-Zurita J, Morales-Nin B (2010) Ecomorphological trends and phylogenetic inertia of otolith sagittae in Nototheniidae. Environ Biol Fish **89**:607–618

Lundberg YW, Xu Y, Thiessen KD, Kramer KL (2015) Mechanisms of otoconia and otolith development. Dev Dynam **244**(3):239–253

Mac Arthur RH (1972) Geographcal ecology: patterns in the distribution of species. Harper and Row, New York, 269 p

Mendoza RPR (2006) Otoliths snd their applicationsin fishery science. Croat J Fish **64**(3):89–102

Meyer-Rochow VB (1999) Comming to grips with a slippery issue: human waste disposal in cold climates. Int J Circumpol Heal **58**:57–62

Meyer-Rochow VB, Cook I, Hendy CH (1992) How to obtain clues from the otoliths of an adult fish about the aquatic environment it has been in as a larva. Comp Biochem Phys A **103**:333–335

Militelli MI, Macchi GJ, Rodrigues KA (2015) Maturity and fecundity of *Champsocephalus gunnari, Chaenocephalus aceratus* and *Pseudochaenichthys georgianus* in South Georgia and Shag Rocks Islands. Polar Sci **9**:258–266

Miller JA, Hurst TP (2020) Growth rate, ration, and temperatur effects on otolith elemental incorporation. Front Mar Sci **7**:320. doi:10.3389/fmars.2020.00320

Miyazaki T, Iwami T, Meyer-Rochow VB (2011) The position of the retinal area centralis changes with age in *Champsocephalus gunnari* (Channichthyidae), a predatory fish from coastal Antarctic waters. Polar Biol **34**:1117–1123

Montgomery JC, Coombs S, Janssen J (1994) Form and function relationships in lateral line systems: comparative data from six species of Antarctic notothenioid fish. Brain Behav Evol **44**:299–306

Montgomery JC, Macdonald JA (1987) Sensory tuning of lateral line receptors in Antarctic fish to the movements of planktonic prey. Science **235**:195–196

Montgomery JC, Macdonald JA, Housley GD (1988) Lateral line function in an Antarctic fish related to the signals produced by planktonic prey. J Comp Physiol A **163**:827–833

Morris RW, Kittleman LR (1967) Piezoelectric property of otoliths. Science **158**(3799):368–370. doi:10.1126/science.158.3799.368

Motta CM, Bice A, Balassone G, Balsamo G, Fascio U, Simoniello P, Tammaro S, Marmo F (2009) Morphological and biochemical analyses of otoliths of the ice-fish *Chionodraco hamatus* confirm a common origin with red-blooded species. J Anat **214**(1):153–162. doi:10.1111/j.1469-7580.2008.01003.x

Mucha M (1980) Characteristics of South Georgia icefish (*Pseudochaenichthys georgianus*, Norman) from the region of South Georgia Island (Antarctic) in the years 1977–1979. Pol Polar Res **1**(4):163–172

North AW (1988) Distribution of fish larvae at South Georgia: horizontal, vertical and temporal distribution and early life history relevant to monitoring year-class strength and recruitment. Commission for the Conservation of Antarctic

Marine Living Resources, Hobart, pp 105–142

North AW (1990) Ecological studies of Antarctic fish with emphasis on early development of inshore stages at South Georgia. University of Hull, Ph.D. Thesis, pp 1–319

North AW, White MG (1987) Reproductive strategies of Antarctic fish. In: Kullander SO, Fernholm B (eds), Proc Vth Congress of European Ichthyology. Swedish Museum of Natural History, Stockholm, pp 381–390

Parmentier E, Cloots R, Warin R, Henrist C (2007) Otolith crystals (in Carapidae): Growth and habit. J Struct Biol **159**:462–473

Permitin JE (1973) Plodovitost i biologija rozmnozenija belokrovych (sem. Chaenichthyidae), ugretreskovych (sem. Muraenolepidae) i antarkticeskich ploskonosov (sem. Bathydraconidae) moria Skorza (Antarktika). *Voprosy Ichtiologii*, **13**:245–258

Popper AN, Hawkins AD, Sand O, Sisneros JA (2019) Examining the hearing abilities of fishes. J Acoust Soc Am **146**(2):948–955

Radtke RL, Hourigan TF (1990) Age and Growth of the Antarctic fish *Nototheniops nudifrons*. Fish B-NOAA **88** (3):557–571

Reid K (2017) Peer-review of fisheries management in the commission for the Conservation of Marine Living Resources (CCAMLR). In: American Fisheries Society 147 Annual Meeting, Tampa, 20–24 Aug 2017, 110 p

Reimer T, Dempster T, Warren-Myers F, Jensen A, Swearer S (2016) High prevalence of vaterite in sagittal otoliths causes hearing impairment in farmed fish. Sci Rep **6**:25249. doi:10.1038/srep25249

Salim SA, Thekra LI (2009) Solving linear programming problems by using Exscel's solver. Tikrit J Pure Sci **14**:1–12

Schulz-Mirbach T, Ladich F, Plath M, Hess M (2019) Enigmatic ear stones: what we know about the functional role and evolution of fish otoliths. Biol Rev **94**:457–482

Sheykholeslami K, Kaga K (2002) The otolithic organ as a receptor of vestibular hearing revealed by vestibular-evoked myogenic potentials in patients with inner ear anomalies. Hearing Res **165**(1–2):62–67

Sobczak R, Nitkiewicz Z, Koszkul J (2003) Supermolecular structure and thermal properties of polypropylene composites reinforced glass fibre (Struktura nadcząsteczkowa i własności termiczne kompozytów na osnowie polipro pylenu wzmacnianych włóknem szklanym). Kompozyty, **3**(8):343–348

Sosiński J, Paciorkowski A (1993) State of mackerel icefish (*Champsocephalus gunnari* Lonnberg, 1905) stock from South Georgia area based on Polish biological investigationsin 1975–1992. Pol Polar Res, **14**:407–431

Thomas ORB, Swearer SE, Kapp EA, Peng P, Tonkin-Hill GQ, Papenfuss A, Roberts A, Bernard P, Roberts BR (2019) The inner ear proteome of fish. FEBS J **286**(1):66–81

Tomchik SM, Lu Z (2005) Octavolateral projections andorganization in the medulla of a teleost fish, the sleeper goby (*Dormitator latifrons*). J Comp Neurol **481**(1):96–117. doi:10.1002/cne.20363

Traczyk R (2015) Age, growth and distribution of thr Antarctic fish *Pseudochaenichthys georgianus* based on otolith morphometry. Journal of Environmental Science and Engineering **B4**:53–102

Traczyk R, Meyer-Rochow VB (2019) Age structure and biomass of the icefish *Pseudochaenichthys georgianus* Norman (Channichthyidae) between 1976 and 2009: a possible link to climate change. Ocean Polar Res **41**(4): 233–250

Traczyk R, Meyer-Rochow VB, Hughes RM (2020) Icefish Adaptations to climate change on the South Georgia Island Shelf (Sub-Antarctic). Ocean Sci J **55**(2):303–319. doi:10.1007/s12601-019

Traczyk R, Meyer-Rochow VB, Hughes RM (2021) Age determination in the icefish *Pseudochaenichthys georgianus* (Channichthyidae) based on multiple methods usig otoliths. Aquat Biol **30**:1–18

Vanella FA, Calvo J, Morriconi E, Aureliano D (2005) Somatic energy content and histological analysis of the gonads in Antarctic fish from the Scotia Arc. Sci Mar **69**:305–316

Volpedo AV, Echevarría DD (2003) Ecomorphological patterns of the sagitta in fish on the continental shelf off Argentine. Fish Res **60**:551–560

Volpedo AV, Tombari AD, Echeverria DD (2008) Eco-morphological patterns of the sagitta of Antarctic fish. Polar Biol **31**:635–640

Whitehouse MJ, Meredith MP, Rothery P, Atkinson A, WardP, Korb RE (2008) Rapid warming of the ocean around South Georgia, Southern Ocean, during the 20th centuary: forcing, characteristics and implications for lower trophic levels. Deep-Sea Res **55**(1):1218–1228

Wróblewski AK (1983) Encyklopedia fizyki współczesnej. Published by Państwowe Wydawnictwo Naukowe. Państwowe Wydawnictwo Naukowe, Warszawa, 1007 p

Yang T, Hu L, Xiong X, Petru M, Noman MT, Mishra R, Militky J (2020) Sound absorption properties of natural fibers: a review. Sustainabil **12**:8477. doi:10.3390/su12208477

Żabrowski M (2000) The osteology and ossification variability of the skull of antarctic white-blooded fish *Chaenodraco*

wilsoni Regan, 1914 (Channichthyidae, Notothenioidei). Acta Ichthyol Piscat **30**(2):111−126

Zhou G-T, Yao Q-Z, Fu SQ, Guan Y-B (2010) Controlled crystallization of unstable vaterite with distinct morphologies and their polymorphic transition to stable calcite. Eur J Mineral **22**(2):259−269. doi:10.1127/0935-1221/2009/0022-2008

Zhou Q, Lam KH, Zheng H, Qiu W, Shung KK (2014) Piezoelectric single crystalsfor ultrasonic transducers in biomedical applications. Progress in Materials Science **66**:87−111

Author's Information

Ryszard Traczyk
Research Scientist, University of Gdańsk

Victor Benno Meyer-Rochow
Docent, Oulu University
Visiting Professor, Andong National University

Received Dec. 1, 2021
Revised Jan. 24, 2022
Accepted Jan. 24, 2022